Articles

Effect of Surfactant Conformation on the Structures of Small Size Nonionic Reverse Micelles: A Molecular Dynamics Simulation Study

Stéphane Abel,*[,†,‡] Marcel Waks,[‡] Massimo Marchi,[†] and Wladimir Urbach[§,||]

Commissariat à l'Energie Atomique, DSV-DBJC-SBFM, Centre d'Etudes, Saclay, 91191 Gif-sur-Yvette Cedex, France, Laboratoire d'Imagerie Paramétrique, CNRS, UMR7623 LIP, Paris F-75006, France, Université Pierre et Marie Curie Paris 6, Paris F-75005, France, Laboratoire de Physique Statistique, CNRS, UMR8550, Ecole Normale Supérieure, 24 Rue L'homond, F-75231 Paris Cedex 05, France, and UFR Biomédicale, Université Paris 5, 45 Rue des St Pères, 75006 Paris Cedex 06, France

Received April 11, 2006. In Final Form: August 1, 2006

We used constant pressure ($P = 0.1$ MPa) and temperature ($T = 298$ K) molecular dynamics simulations to study the structures and dynamics of small size reverse micelles (RMs) with poly(ethylene glycol) alkyl ether (C_mE_n) surfactants. The water-to-surfactant molar ratio was 3, with decane as the apolar solvent. We focused on the effect of the two possible imposed conformations (trans vs gauche) for the surfactant headgroups on RMs structures and water dynamics. For this purpose, we built up two RMs, which only differ by their surfactant headgroup conformations. The results obtained for the two RMs were compared to what is known in the literature. Here, we show that the surfactant headgroup conformation affects mainly the water-related properties such as the water core size, the area per surfactant headgroup, the headgroup hydration, and the water core translational diffusion. The properties computed for the RM with the surfactant in trans conformation fit better with the experimental data than the gauche conformation. We further show that the surfactant hydrophilic headgroup plays a crucial role in the micellar structures, favors the entrapment of the micellar water, and reduces strongly their diffusion compared to the bulk water.

I. Introduction

Nonionic surfactant systems, in particular those containing the poly(ethylene glycol) alkyl ether, C_mE_n (m = number of carbons in the alkyl chain, n = number of oxyethylene groups) or ($C_mH_{2m+1}(OC_2H_4)_nOH$) can form various phases (i.e. lamellar, hexagonal, micellar, etc.) depending on experimental parameters (such as the hydrophobic and hydrophilic chains length, temperature, or the concentration of the solvent).[1−7] In aqueous solution and above the critical micelle concentration (CMC), surfactants molecules aggregate in regular micelles, widely studied both experimentally and theoretically. In apolar solvents, nonionic surfactants form thermodynamically stable and isotropic water-in-oil microemulsions (W/O) which are able to solubilize large amounts of water in their core.[8] In comparison with ionic surfactant W/O microemulsions such as sodium di-2(ethylexylsulfosuccinate, AOT) which are well-known and widely characterized with various experimental techniques (see ref 9 for data and references), less information on non-ionic microemulsion structures and interiors exists.

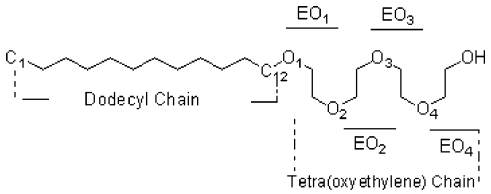

Figure 1. Chemical formula of the *n*-dodecyl tetraoxyethylene glycol monoether ($C_{12}E_4$) surfactant with its different oxyethylene units.

For example, using time-resolved fluorescence quenching methods (TRFQ) spectroscopy in association with dynamic light scattering (DLS), Vasilescu et al.[5] show that Brij-30 reverse micelles (i.e. a commercial analogue of the $C_{12}E_4$ surfactant, Figure 1) grow spherically in cyclohexane, in contrast to decane or dodecane where $C_{12}E_4$–RM become anisotropic with increasing water content.

Other spectroscopic methods (such as NMR,[10,11] ESR-spin probe[12−14]) and ultrasound measurements[15] indicate that water

* Corresponding author: stephane.abel@lip.bhdc.jussieu.fr.
† Commissariat à l'Energie Atomique.
‡ Laboratoire d'Imagerie Paramétrique, CNRS, and Université Pierre et Marie Curie Paris 6.
§ Laboratoire de Physique Statistique, CNRS.
|| UFR Biomédicale, Université Paris 5.

(1) Kunieda, H.; Nakamura, K.; Davis, H. T.; Evans, D. F. Formation of Vesicles and Microemulsions in a Water Tetraethylene Glycol Dodecyl Ether Dodecane System. *Langmuir* **1991**, *7* (9), 1915−1919.
(2) Mitchell, D. J.; Tiddy, G. J. T.; Waring, L.; Bostock, T.; McDonald, M. P., Phase behavior of polyoxyethylene surfactants with water. Mesophase structures and partial miscibility (cloud points). *J. Chem. Soc., Faraday Trans. 1* **1983**, *79* (4), 975−1000.
(3) Olsson, U.; Würz, U.; Strey, R. Cylinders and Bilayers in Ternary Nonionic Surfactant System. *J. Phys. Chem.* **1993**, *97*, 4535−4539.
(4) Olsson, U.; Shinoda, K. B., L. Change of the structure of microemulsions with the hydrophile-lipophile balance of nonionic surfactant as revealed by NMR self-diffusion studies *J. Phys. Chem.* **1986**, *90* (17), 4083−4088.
(5) Vasilescu, M.; Caragheorgheopol, A.; Almgren, M.; Brown, W. A., J.; Johannsson, R., Structure and Dynamics of Nonionic Polyoxyethylenic Reverse Micelles by Time-Resolved Fluorescence Quenching. *Langmuir* **1995**, *11*, 2893.
(6) Shimobouji, T.; Matsuoka, H.; Ise, N.; Oikawa, H. Small-Angle X-ray Scattering Studies on Nonionic Microemulsions. *Phys. Rev. A* **1989**, *39* (8), 4125.
(7) Zana, R.; Weill, C. Effect of the temperature on the aggregation behaviour of nonionic surfactant in aqueous solution. *J. Phys. Lett.* **1985**, *46*, 953−960.
(8) Aveyard, R.; Binks, B. P.; Fletcher, P. D. I.; Ye, X. L. Solubilization of Water in Alkanes Using Nonionic Surfactants. *J. Chem. Technol. Biotechnol.* **1992**, *54* (3), 231−236.
(9) De, T. K.; Maitra, A. Solution Behavior Of Aerosol Ot In Nonpolar-Solvents. *Adv. Colloid Interface Sci.* **1995**, *59*, 95−193.
(10) Tasaki, K.; Abe, A. NMR studies and conformational energy calculations of 1,2-dimethoxyethane and poly(oxyethylene). *Polym. J.* **1985**, *17* (4), 641−55.

10.1021/la060978v CCC: $33.50
Published on Web 09/21/2006

confined in the polar core of small nonionic reverse micelles (RMs) differs from the water in ionic RMs and displays three different states depending on the water content of the micelle (i.e. water trapped in EO groups, bound water next to EO group, and bulklike water).

In the past few years, molecular dynamics (MD)[16] and Monte Carlo[17] simulations have been successfully used to study poly(ethylene oxide) chains in water or nonionic surfactants in various mesophases (air/water interface,[18,19] lamellar,[20] or micellar phases[21−23]). All these studies emphasize the fact that the surfactant hydrophilic headgroup conformation (the oxyethylene (EO) part) depends on its hydration[24] and favor the gauche helix form rather than the trans, in agreement with experimental observations of similar systems.[25,26]

In contrast to other ionic surfactants (such as AOT,[27,28] carbonate calcium,[29] or fluoro-based surfactants[30−32]), only one molecular dynamics study of nonionic reverse micelles has been performed.[33] The authors report the structure of a united atom model of a short nonionic surfactant ($C_{12}E_2$) RM in decane with a surfactant-to-water molar ratio ($W_o = [H_2O]/[C_{12}E_2]$) close to 2.4. Despite the low value of W_o, they showed that the core water molecules interact strongly with the oxyethylene headgroups and favor the gauche conformation as reported for other phases (such as air/water interface, lamellar phases, or micellar phases).

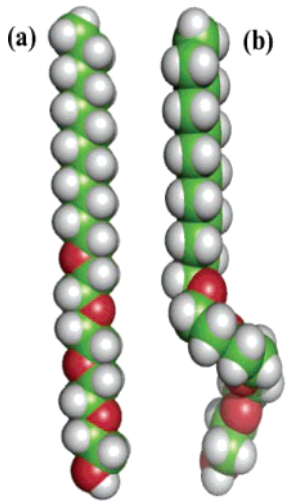

Figure 2. $C_{12}E_4$ surfactant molecule in "all-trans" (RM94t) (a), and in gauche "helix" (RM94g) (b) conformations. See main text for explanations. Atoms are drawn in CPK style. Carbons, hydrogen, and oxygen atoms are green, white, and red, respectively. These pictures were produced with Pymol software.[59]

Structural data of small RMs with intermediate chain length surfactant (i.e. $C_{12}E_4$) with poor water content are more sporadic, and several questions remain to be answered. Is the EO intermediate chain of the $C_{12}E_4$ adopting the same gauche conformation as reported for $C_{12}E_2$ RM despite the low quantity of water in the micellar core? And if the gauche conformation exists in small RM, what is its effect (compared to trans conformation) on the micelle and water core structures?

Here we report, two 3 ns (for a total 6 ns) MDs of $C_{12}E_4$ RM with a water-to-surfactant molar ratio, $W_o = [H_2O]/[C_{12}E_4]$, of 3. We compare the effect of two initial conformations (extended vs gauche) for the $C_{12}E_4$ EO headgroups on the structural and dynamic properties of the aggregates.

This article is organized as follows: In the next sections, we will discuss the construction of our models of RMs and the potential used to model our systems. This will be followed by section covering the MD procedures, the results, and the interpretations of our simulations.

II. Methods

Construction of Reverse Micelles. In this work, the two RMs consist each of 94 surfactant molecules each, with two different conformations for the hydrophilic group. The first named RM94t was started with 94 molecules in the extended (i.e. "all trans") conformation (Figure 2a), whereas the second RM94g has its surfactant molecules in the gauche (i.e. 'helix") conformation for the hydrophilic group (Figure 2b). The gauche conformation for the surfactant headgroup was modeled by giving to the three first OCCO dihedral angles (near the dodecane chain, Figure 2b) a gauche$^-$ conformation and for the last OCCO and four COCC a trans conformation.[16]

(11) Kawai, T.; Shindo, N.; K., k.-n. Solubilized states of water and formation of reversed micelles in polyoxyethylated nonylphenyl ethers in cyclohexane media. *Colloid Polym. Sci.* **1995**, *195* (2), 195.
(12) Caldararu, H.; Caragheorgheopol, A.; Vasilescu, M.; Dragutan, I.; H., L. Structure of the Polar Core in Reverse Micelles of Nonionic Poly(oxyethylene) Surfactants, As Studied by Spin Probe and Fluorescence Probe Techniques. *J. Phys. Chem.* **1994**, *98* (20), 5320−5331.
(13) Pant, D.; Levinger, N. E. Polar Solvation Dynamics in Nonionic Reverse Micelles and Model Polymer Solutions. *Langmuir* **2000**, *16* (26), 10123−10130.
(14) Qi, L. M.; Ma, J. M. Investigation of the microenvironment in nonionic reverse micelles using methyl orange and methylene blue as absorption probes. *J. Colloid Interface Sci.* **1998**, *197* (1), 36−42.
(15) Amararene, A.; Gindre M.; Le Huérou, J.-Y.; Nicot, C.; Urbach, W.; Waks, M. Water Confined in Reverse Micelles: Acoustic and Densimetric Studies. *J. Phys. Chem. B* **1997**, *101* (50), 10751−10756.
(16) Tasaki, K. Poly(oxyethylene)-Water Interactions: A Molecular Dynamics Study. *J. Am. Chem. Soc.* **1996**, *118*, 8459.
(17) Engkvist, O.; Karlstrom, G. Monte Carlo Simulation Study of Short Poly(ethylene oxide) Chains at Different Concentrations. *J. Phys. Chem. B* **1997**, *101* (9), 1631−1633.
(18) Kuhn, H.; Rehage, H. Molecular dynamics computer simulations of surfactant monolayers: Monododecyl pentaethylene glycol at the surface between air and water. *J. Phys. Chem. B* **1999**, *103* (40), 8493−8501.
(19) Chanda, J.; Bandyopadhyay, S. Molecular Dynamics Study of a Surfactant Monolayer Adsorbed at the Air/Water Interface. *J. Chem. Theory Comput.* **2005**, *1* (5), 963−971.
(20) Bandyopadhyay, S.; Tarek, M.; Lynch, M. L.; Klein, M. L. Molecular dynamics study of the poly(oxyethylene) surfactant $C_{12}E_2$ and water. *Langmuir* **2000**, *16* (3), 942−946.
(21) Sterpone, F.; Briganti, G.; Pierleoni, C., Molecular Dynamics Study of Spherical Aggregates of Chain Molecules at Different Degrees of Hydrophilicity in Water Solution. *Langmuir* **2001**, *17* (16), 5103−5110.
(22) Sterpone, F.; Pierleoni, C.; Briganti, G.; Marchi, M. Molecular Dynamics Study of Temperature Dehydration of a C12E6 Spherical Micelle. *Langmuir* **2004**, *20* (11), 4311−4314.
(23) Garde, S.; Yang, L.; Dordick, J. S.; Paulaitis, M. E. Molecular dynamics simulation of C8E5 micelle in explicit water: structure and hydrophobic solvation thermodynamics. *Mol. Phys.* **2002**, *100* (14), 2299−2306.
(24) Yoshida, H.; Takikawa, K.; Kaneko, I.; Matsuura, H. Conformational Analyses of Model Compounds of Nonionic Surfactants in Aqueous Solution: Raman Spectroscopy and ab initio MO Calculations *J. Mol. Struct.* **1994**, *311*, 205−210.
(25) Viti, V.; Indovina, P. L.; Podo, F.; Radics, L.; Némethy, G. Conformational studies of ethylene glycol and its two ether derivatives II. A nuclear magnetic resonance study of 3-methoxyethanol and 1,2-dimethoxyethane. *Mol. Phys.* **1974**, *27*(2), 541−559.
(26) Matsuura, H. F., K., Conformational analysis of poly(oxyethylene) chain in aqueous solution as a hydrophilic moiety of nonionic surfactants. *J. Mol. Struct.* **1985**, *126*, 251−260.
(27) Abel, S.; Sterpone, F.; Bandyopadhyay, S.; Marchi, M. Molecular Modeling and Simulations of AOT-Water Reverse Micelles in Isooctane: Structural and Dynamic Properties. *J. Phys. Chem. B* **2004**, *108* (50), 19458−19466.
(28) Faeder, J.; Ladanyi, B. M., Molecular Dynamics Simulations of the Interior of Aqueous Reverse Micelles. *J. Phys. Chem. B* **2000**, *104* (5), 1033−1046.
(29) Tobias, D. J.; Klein, M. L. Molecular dynamics simulations of a calcium carbonate calcium sulfonate reverse micelle. *J. Phys. Chem.* **1996**, *100* (16), 6637−6648.
(30) Senapati, S.; Berkowitz, M. L. Molecular Dynamics Simulation Studies of Polyether and Perfluoropolyether Surfactant Based Reverse Micelles in Supercritical Carbon Dioxide. *J. Phys. Chem. B* **2003**, *107* (47), 12906−12916.
(31) Senapati, S.; Berkowitz, M. L. Water structure and dynamics in phosphate fluorosurfactant based reverse micelle: A computer simulation study. *J. Chem. Phys.* **2003**, *118* (4), 1937−1944.
(32) Salaniwal, S.; Cui, S. T.; Cummings, P. T.; Cochran, H. D. Self-assembly of reverse micelles in water/surfactant/carbon dioxide systems by molecular simulation. *Langmuir* **1999**, *15* (16), 5188−5192.
(33) Allen, R.; Bandyopadhyay, S.; Klein, M. L. $C_{12}E_2$ Reverse Micelle: A Molecular Dynamics Study. *Langmuir* **2000**, *16* (26), 10547−10552.

The number of surfactant molecules per RM (N_{C12E4}) was estimated by Vasilescu et al.,[5] based on the TRFQ method at 298 K. This technique determines N_{C12E4} and derives the radius of the polar core R_{pc} according to the following formula:[5]

$$R_{pc}{}^3\,(\text{Å}^3) = \frac{3N_{C12E4}}{4\pi}(V_{EO} + V_{H2O}) = \frac{262.8 + 30W_o}{4.19}N_{C12E4} \quad (1)$$

Here, V_{EO} and V_{H2O} are the estimated molecular volumes obtained from the densities of the headgroup $(OC_2H_4)_4OH$ and water, respectively.

From the curve at 25 °C of N_{C12E4} as a function of W_0 of ref 3, we have estimated $N_{C12E4} = 114$ for $W_0 = 3$. On the other end, if the value of R_{pc} (20.6 Å) is used from the SAXS experiment by Valdez,[34] we find $N_{C12E4} = 104$. To reduce the system size of our simulations, we took a value of $N_{C12E4} = 94$. This is smaller than that obtained from the TRFQ and SAXS experiments, but well within their experimental error between 10 and 20% for similar systems (see paper by Clark et al.[35] for a discussion on the TRFQ errors).

The number of solvent molecules and the size of the simulation box were chosen to be compatible with a "L_2" phase of RM and to be in a similar concentration as in the Vasilescu work[5] (i.e. a weight/weight (w/w) ~85% of oil).

For the simulations presented in this paper, we have adopted an all atom potential for $C_{12}E_4$, decane, and water. The force field topology and parameters used to model the system originate from different sources. For the dodecyl chain, the alcoholic group of the surfactant and for the solvent, we used the bonded and nonbonded parameters available in CHARMM.[36] For the hydrophilic part of the surfactant, we used the force field of Tasaki, initially parametrized for a single PEO chain in water.[16] To mimic the micellar water, we used the SPC water model,[37] in agreement with the original description.[16]

The preparation and the equilibration procedures of the two micelles were as follows: first we have constructed a spherical cluster of 282 water molecules from the final configuration of a 100 ps MD runs of 512 SPC bulk water molecules simulated in a cubic box at $T = 300$ K and $P = 0.1$ MPa. The corresponding numbers of surfactant in extended and gauche conformations were placed by hand around a sphere, the dodecane tail (C_{12}) pointing toward the exterior and with the nearest oxygen atom (O_1) at the distance R_{pc} from the center. Following this step, the two systems were equilibrated at 500 K in a vacuum during 500 ps with a spherical cutoff of 10 Å, keeping the hydrophilic group of the surfactant and the water in order to randomize the hydrophobic chain of the surfactant. Subsequently, each system was inserted in an octahedron box with an appropriate size and filled with the adequate number of decane molecules to ensure a mass fraction of solvent close to 85% for an L_2 phase for this ternary system (see Table 1 for the summary of the RM's initial parameters of each system). After this step, the system was equilibrated at 450 K for 300 ps, to relax the hydrophobic chain of $C_{12}E_4$ and the solvent molecules. At this point the water and the headgroups were unblocked and the system was then frozen at 0 K. The temperature of each system was monotonically increased to 300 K in 300 ps as described in ref 27. The resulting configurations were simulated in NPT ensemble ($T = 298$ K and $P = 0.1$ MPa) for 3 ns after a 70 ps equilibration period. The system atomic coordinates were saved once every 240 fs for subsequent analysis.

Molecular Dynamics. To simulate in the NPT ensemble, we used a method based on the extended system approach.[38−41] This technique involves adding extra (virtual) dynamical variables to the system coordinates and momenta in order to control temperature and pressure. To integrate the equation of motion, we used a five time step r-RESPA (reversible reference system propagation algorithm) integrator with a 12 fs time step, as described elsewhere.[42] It was combined with a smooth particle mesh Ewald (SPME)[43] to handle electrostatic interactions and constraints on covalent bonds entailing hydrogens.

Table 1. Simulation Initial Parameters[a]

system	RM94t	RM94g
W_o	3	3
N_{C12E4}	94	94
N_{H2O}	282	282
N_{DEC}	1612	1607
m_{DEC}/m_{Total}	85.4	85.3
N_{atm}	58728	58568
R_{pc} (Å)	20.0	20.0
A_h (Å^2)	53.5	53.5
t (ns)	3.0	3.0

[a] N_{C12E4}, N_{H2O}, and N_{DEC} are the numbers of $C_{12}E_4$, water, and decane molecules composing the simulated systems. m_{DEC}/m_{Total} is the mass fraction of decane in the system (% w/w). N_{atm} gives the total number of atoms in the simulation box. R_{pc} is the initial radius of the polar core. A_h is the initial surface area per surfactant, and t is the simulation duration, not including the 70 ps equilibration period.

The SPME parameters were chosen to maintain for the all the RM systems a relative error on the electrostatic interaction < 0.1%. For this purpose, we used a convergence parameter $\alpha = 0.43$ Å^{-1}, a fifth-order B-spline and a 100-point grid in each Cartesian direction to take care of the SPME charge interpolation. As in ref 27, all our systems were simulated in a periodically replicated primitive body center cubic (bcc) box corresponding to a system with truncated octahedral boundary conditions. The sequential version of the program ORAC[44] was used throughout this work to perform simulation and analyses of the atomic trajectories.

To compare the effect of the water in the micelle cores with the bulk we have also carried out an additional simulation in the NPT ensemble of 2197 SPC water molecules, at $T = 298$ K and $P = 0.1$ MPa, and for 1 ns.

As shown in Table 2, the average volumes of the two systems are similar 611745 ± 1813 Å^3 and 610435 ± 1843 Å^3. The solvent volume fractions for the two systems are close to ~88.2%, in agreement with a well-defined "L_2" phase. We point out that the average density is identical for the two systems ($\rho = 0.73 \pm 0.01$ g/cm^3).

III. Results

Size and Shape of the Micelles. We first focus on the shape and the size of the two reverse micelles. As shown in Figure 3 and Table 3, the micelles present a deviation from the sphericity. To quantify the extent of this deviation for each RM, we have computed from the MD trajectories the three semi-axes *a*, *b*, and *c* lengths obtained from the inertia tensor (see ref 27 for details on the calculation) of an ellipsoid of identical mass. To monitor

(34) Valdez, D. Compressibilité des milieux confinés: micelles inverses et protéines. Etude d'hydratation controlée. Ph.D. Thesis, Université Pierre et Marie Curie Paris VI, Paris, 2001.

(35) Clark, S.; Fletcher, D. I. P.; Ye, X. Interdroplet exchange rates of water-in-oil and oil-in-water microemulsion droplets stabilized by pentaoxyethylene monododecyl ether. *Langmuir* **1990**, *6* (7), 1301−1309.

(36) MacKerell, J. A. D.; Brooks, B.; Brooks, I. C. L.; Nilsson, L.; Roux, B.; Won, Y.; Karplus, M. *CHARMM: The Energy Function and Its Parameterization with an Overview of the Program*; John Wiley & Sons: Chichester, 1998; Vol. 1, pp 271−277.

(37) Berendsen, H. J. C.; Postma, J. P. M.; Van Gunsteren, W. F.; Hermans, J. In *Intermolecular Forces*; Pullman, B., Ed.; Reider: Dodrecht, 1981.

(38) Andersen, H. C. Molecular dynamics simulations at constant pressure and/or temperature. *J. Chem. Phys.* **1980**, *72* (4), 2384−2393.

(39) Parrinello, M.; Rahman, A. Polymorphic transitions in single crystals: A new molecular dynamics method. *J. Appl. Phys.* **1981**, *52* (12), 7182−7190.

(40) Nose, S. A molecular dynamics method for simulations in the canonical ensemble. *J. Chem. Phys.* **1984**, *52* (2), 511−519.

(41) Hoover, W. G. Canonical dynamics: Equilibrium phase-space distributions. *Phys. Rev. A* **1985**, *31* (3), 1695−1697.

(42) Marchi, M.; Procacci, P. Coordinates scaling and multiple time step algorithms for simulation of solvated proteins in the NPT ensemble. *J. Chem. Phys.* **1998**, *109*(13), 5194−5202.

(43) Essmann, U.; Perera, L.; Berkowitz, M. L.; Darden, T.; Lee, H.; Pedersen, L. G. A smooth particle mesh Ewald method. *Chem. Phys.* **1995**, *103*, 8577−8594.

(44) Procacci, P.; Darden, T. A.; Paci, E.; Marchi, M. ORAC: A molecular dynamics program to simulate complex molecular systems with realistic electrostatic interactions. *J. Comput. Chem.* **1997**, *18*, 1848.

Table 2. Cell Averaged Parameters[a]

system	RM94t	RM94g
$\langle a_{to} \rangle$	80.25	80.15
$\langle V_{cell} \rangle$	611745	610435
σ_{Vcell}	1813	1843
ϕ_{C12E4}	10.3	10.3
ϕ_{H2O}	1.4	1.4
ρ	0.73	0.73

[a] The symbol $\langle ... \rangle$ stands for ensemble average. $\langle a_{to} \rangle$ gives the cell parameter (Å) of the truncated octahedron simulation cell. $\langle V_{cell} \rangle$ is the cell volume (Å^3) average and σ_{Vcell} its standard deviation. ϕ_{C12E4} and ϕ_{H2O} are the volume fractions (%) of surfactant and water in the system, respectively. ρ is the averaged density (g/cm^3) of the system. The statistical error on density is less than 1.5%.

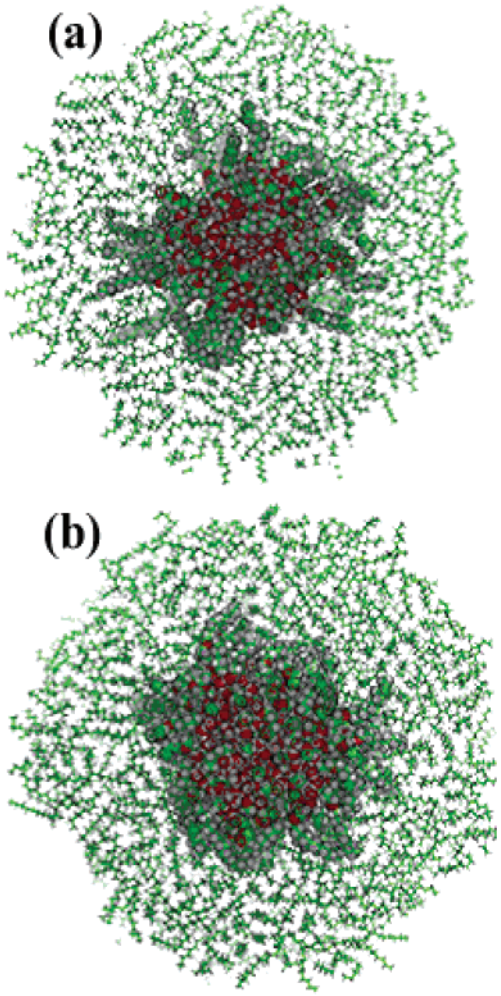

Figure 3. View of $C_{12}E_4$ inverted micelles in decane at the end of the simulation. We present a view of the simulation box clipped by a plane orthogonal to the *X*-axis and crossing the center of mass of the $C_{12}E_4$-water micelle. Panel a: RM94t. Panel b: RM94g. The atoms of the $C_{12}E_4$ chain and water are represented by spheres, whereas the decane covalent bonds are shown as lines. In the picture, carbon atoms are green, hydrogen atoms gray, and oxygen atoms red. These pictures were produced with Pymol.[59]

the aggregates stability vs the time, we have also computed the instantaneous eccentricities of the RMs and of their water core during the simulation. As shown in Figure 4, RM94t presents a stable ellipsoidal shape for the entire micelle (in black) and its water core (in red) after ~700 ps of simulation. For RM94g, the shape of the water is also stable after 700 ps of calculation, but we observe more thermal fluctuations than for RM94t during the production run since the water exists in a more free form (see above). In Table 3, we have computed the average ratio between the major and the minor semi axis *a*/*c* and the average eccentricity, *e*, for the micelles and for their water cores, after discarding the first 250 ps of the runs.

Table 3. Micelle Shape Parameters[a]

system	a	b	c	*a*/*c*	e
RM94t	30.4 ± 0.3	29.1 ± 0.2	24.5 ± 0.3	1.24 ± 0.02	0.59 ± 0.02
water core	21.8 ± 0.4	18.8 ± 0.4	17.5 ± 0.3	1.24 ± 0.03	0.59 ± 0.03
RM94g	29.7 ± 0.4	26.8 ± 0.4	24.7 ± 0.4	1.20 ± 0.03	0.56 ± 0.03
water core	19.2 ± 1.6	15.9 ± 1.0	11.9 ± 0.4	1.61 ± 0.14	0.78 ± 0.05

[a] The semi axes $a > b > c$ (Å) have been computed from the three moments of inertia and averaged over the trajectories, after discarding the first 250 ps. The eccentricity, *e*, was computed as $e = (1 - (c^2/a^2))^{1/2}$. For a perfect sphere, *e* is zero, whereas $e \rightarrow 1$ for a flat or needlelike shape. Each row of the table labeled with the simulation logo refers to the semi axes of the entire micelle. The "water core" labeled rows report the semiaxes computed only with the water molecules.

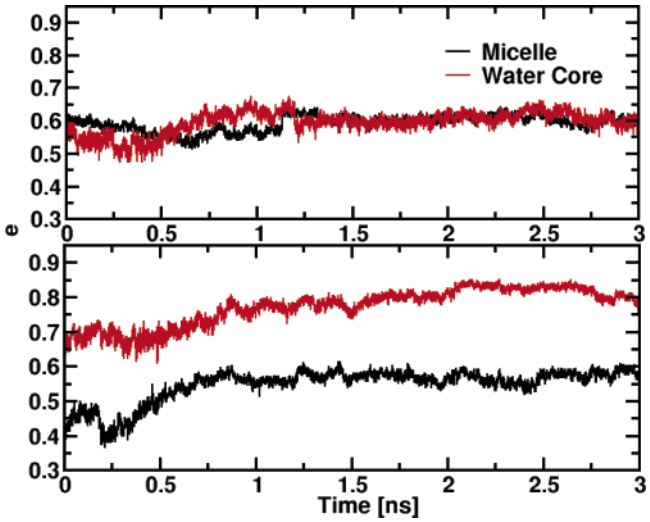

Figure 4. Time evolution of the eccentricity, *e*, for micelles RM94t (top) and RM94g (bottom).

RM94t as well RM94g are "oblate-like" ellipsoids $b \approx c$ within the 3 ns simulations. The average ratio *a*/*c* is close to ~1.24 (i.e. within a statistical error of ± 0.03) whereas *e* is close to 0.59 for each micelle and does not seem to depend on the initial conformation of the surfactant headgroup. In contrast, the water core is more flattened for RM94g ($e = 0.78 \pm 0.05$) than in RM94t ($e = 0.59 \pm 0.03$). This deviation from the sphericity of the both water core shape shows instead the dependence of the initial conformation of the hydrophilic headgroup of $C_{12}E_4$ on the water core properties, as we will find through this paper. As reported in the literature,[5,45] the reverse micellar shape in decane deviates significantly from sphericity at 298 K as the amount of water in the core increases. This can also exist for small size $C_{12}E_4$ RMs (i.e. $W_o \leq 4$)).[5] If we compare with the model of $C_{12}E_2$ RMs in decane of Klein et al.,[33] these authors found a micelle with a spherical shape, and this difference can be due to the surfactant used ($C_{12}E_2$ vs $C_{12}E_4$) or the size of the RMs simulated.

A useful structural parameter to measure the size of the micelle is its radius of gyration, R_g, defined as

$$R_g^2 = \sum_i m_i (r_i - r_{cm})^2 / \sum_i m_i \qquad (2)$$

In this equation, m_i is the mass of the atom *i* at the distance r_i from the center of mass r_{cm} of the aggregate. For a nonspherical object as our micelles, the radius of gyration can be directly

Table 4. Micelle Size Parameters[a]

system	R_g^M	$\bar{R}^M$	R_g^{pc}	R_g^W	$\bar{R}^w$	A_v^h	A_e^h	d_{C12E4}
RM94t	21.8 ± 0.2	27.8 ± 0.3	17.6 ± 0.1	15.0 ± 0.1	19.2 ± 0.4	59.6 ± 0.4	59.2 ± 0.1	23.3
RM94g	21.0 ± 0.2	26.9 ± 0.3	17.5 ± 0.1	12.4 ± 0.7	15.3 ± 0.9	38.3 ± 0.5	37.3 ± 0.1	21.8

[a] The quantities labeled by superscripts M and W were computed by including all atoms of the micelle and those of the water core, respectively. The radii of gyration (Å), R_g, were obtained from the ellipsoid semiaxes reported in Table 3 by using eq 3. The average radius $\bar{R}$ corresponds to the radius of a sphere with the volume identical to the ellipsoids of Table 3. In column 3 are reported the radii of gyration obtained with the eq 2, including the water molecules and the hydrophilic group of the surfactant. In the last two columns, we give the average surface areas (Å^2) per $C_{12}E_4$ molecule in contact with water. A_v^h was derived from the Voronoi construction, whereas A_e^h was computed assuming an ellipsoid-like geometry for the water core (see the text). In the last column, the average end-to-end distances of the $C_{12}E_4$ molecule are reported. This latter quantity has been obtained from the broad peak of the end-to-end probability distribution function (see Figures 7 and 8). All these data have been averaged over all trajectories, after discarding the first 250 ps.

obtained from the semiaxes lengths (a, b, and c) for an ellipsoidal solid with a uniform density, with the following expression:

$$R_g^2 = \frac{a^2 + b^2 + c^2}{5} \tag{3}$$

We verified for our systems that the two definitions of the R_g are equivalent, as the two values never differed from each other more than 2−3% (not shown). Alternative, but more time-consuming, techniques exist in the literature to compute R_g.[46] However, the difference with our mass-weighted R_g does not exceed 5%.

As in our previous work on AOT reverse micelles,[27] we have defined three radii of gyration for each RM depending on the atoms included in eqs 2 or 3: R_g^M including all the atoms of the micelle (surfactant and water), R_g^{pc}, defined by the $(OCH_2)_4OH$ atoms of the $C_{12}E_4$ and the water molecules, and R_g^W including only water atoms. R_g^{pc} was obtained with eq 2, whereas R_g^M and R_g^W were computed with eq 3. As shown in Table 4, and for both micelles: $R_g^M > R_g^{pc} > R_g^W$. The R_g^M values computed for the two micelles are found to be similar. The calculation of the radius polar core R_g^{pc} for both micelles leads also to similar values (∼17.6 ± 0.1 Å). In contrast, we found that the size of the water pool is smaller in RM94g (12.4 ± 0.7 Å) than RM94t (15.0 ± 0.1 Å).

To compare the micellar size of our RMs with sizes obtained from scattering experiments (such as SAXS or SANS), which assume a spherical shape, we have computed the average radius of the RMs $\bar{R}^M$ and that of their water pool ($\bar{R}^W$). $\bar{R}$ corresponds to the radius of the sphere having the same volume as the corresponding inner core ellipsoid (i.e. with water and hydrated headgroup units).[27] This value is obtained from the expression: $\bar{R} = (abc)^{1/3}$. In Table 4, we report values of $\bar{R}^M$ and $\bar{R}^W$, obtained with the ellipsoid semiaxes a, b, and c of the RM and their water pool, presented in Table 3. The value of $\bar{R}^W$ found for RM94t (∼19.2 ± 0.4 Å) is in good agreement with the value of 20.0 Å set while constructing the micelles and close to the experimental values of the polar core radius measured by Valdez[34] by SAXS for $C_{12}E_4$ RM in decane with $W_o = 3$ (20.6 ± 1.0 Å) or estimated from Ravey et al.[45] by SANS (18.4 Å). In contrast for RM94g, the computed $\bar{R}^W$ gives a value ∼25.3% smaller than the experiment values.[5,34]

In the sixth and seventh columns of Table 4, we have reported the surface area per surfactant around the water core (A^h). The A_e^h for both micelles were obtained by computing the surface area of the water core approximated to an ellipsoidal shape and divided by the number of surfactant molecules N_{C12E4}. A_v^h was instead computed with the Voronoi construction[47] by adding up the surface area of each Voronoi polyhedron[48] shared between the hydrophilic group of the surfactant and the water. With the latter surface, we obtain a direct value of the surface contact between the surfactant headgroup atoms and the water molecules. For RM94t, we found that $A_e^h = 59.2 \pm 0.1$ Å^2 and $A_v^h = 59.6 \pm 0.4$ Å^2. These values agree well with the values estimated from Ravey et al.[45] by SANS (∼57.5 Å^2) or obtained by Valdez[34] by SAXS (51.2 ± 0.1 Å^2). In contrast to RM94g, where the values are found ∼1.5 times smaller ($A_v^h = 38.3 \pm 0.1$ Å^2 and $A_e^h = 37.3 \pm 0.1$ Å^2), it should be emphasized that the A^h value is usually calculated assuming a spherical shape for the water core with the expression $A_s^h = 4\pi(\bar{R}^W)^2/N_{C12E4}$. This assumption leads for RM94t an $A_s^h = 49.2 \pm 0.1$ Å^2, whereas for RM94g to A_s^h (31.3 ± 0.1 Å^2) still remains far from the experimental values.[45,34] These results suggest that the trans conformation (RM94t) better reproduces the experimental data than the gauche conformation.

Aggregate Microstructure. To obtain more information on the structure and the spatial localization of each component in both micelles, we have computed their radial mass density profiles $\rho_a(r)$ with respect to the center of mass (COM) ($r = 0$ Å) of the aggregates. The averaged $\rho(r)$ was over 3 ns for the water molecules (H_2O), the surfactant hydrophilic headgroup (EO_{1-4}), the terminal hydroxyl groups (OH), the hydrophobic tail (C_{12}), and decane (DEC) are shown in Figures 5 and 6. Remember that the nonspherical nature of our micelles will affect the interpretation of $\rho(r)$ to a certain extent by causing broadening and overlap of these density functions.

We notice that, in both micelles, the water core is protected from oil by the interfacial region limited by the surfactant tetra(oxyethylene) part, which extends from ∼10 to ∼22 Å (see Figures 5 and 6 and insets). The radial profiles of water confirms, as suggested in previous sections (i.e. with the water core sizes), that the two aggregates differ mainly in their water pool. In RM94t, the water molecules are mainly trapped in the EO_{4-2} units of the $C_{12}E_4$. The water density is ∼40% less than in the bulk water due to the penetration of the surfactant hydrophilic headgroups into the water core. In contrast, RM94g's water molecules form a closely packed water pool with an average density close to bulk water (∼1 g/cm^3) at ∼6.0 Å from the center of mass of the aggregate. For both micelles, the broad radial profiles of the aliphatic chain C_{12} extends from ∼20 to ∼32 Å indicating that the dodecyl tail of the $C_{12}E_4$ penetrates deeply into the solvent phase. Further investigation shows that 83% of the total surface of the micelles computed by adding up the surface of the Voronoi facets[47,48] are due to the hydrophobic

(45) Ravey, J. C.; Buzier, M.; Picot, C. Micellar Structures of Nonionic Surfactants in Apolar Media. *J. Colloid Interface Sci.* **1984**, *97* (1), 10.

(46) Merzel, F.; Smith, J. C. SASSIM: a method for calculating small-angle X-ray and neutron scattering and the associated molecular envelope from explicit-atom models of solvated proteins. *Acta Crystallogr. Sect. D* **2002**, *58* (2), 242−249.

(47) Voronoi, G. F. Nouvelles applications des paramètres continus à la théorie des formes quadratiques. *J. Reine Angew. Math.* **1908**, *134*, 198−287.

(48) Procacci, P.; Scateni, R., A General Alglorithm for Computing Voronoi Volumes: Application to the Hydrated Crystal of Myoglobin. *Int. J. Quantum Chem.* **1992**, *42*, 1515−1528.

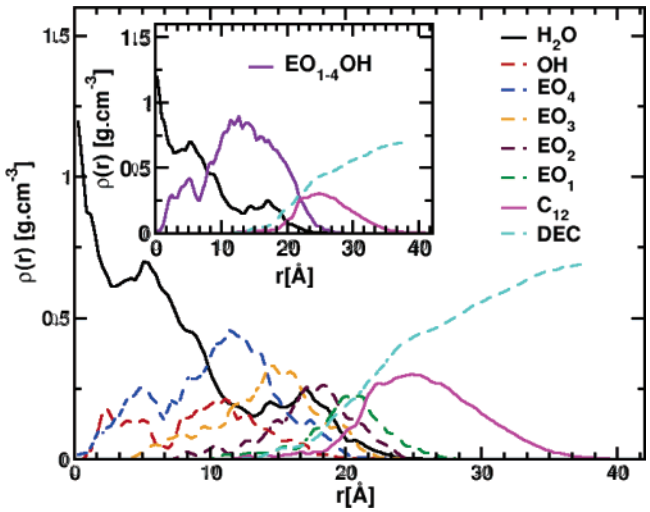

Figure 5. RM94t radial profiles with respect to the center of mass ($r = 0$ Å) of the aggregate. A 0.3 Å bin width was used. In the inset, we have plotted the radial profiles for the whole tetra(oxyethylene) part (purple), dodecane chain (magenta), the water, and decane.

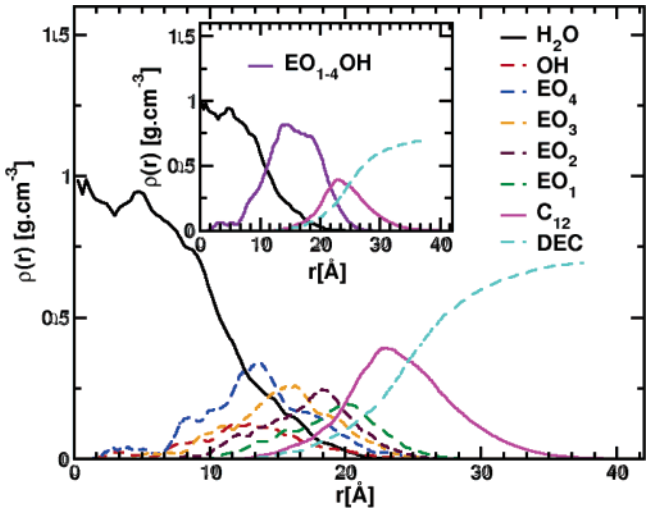

Figure 6. RM94g average radial profiles with respect to the center of mass ($r = 0$ Å) of the aggregate. A 0.3 Å bin width was used. In the inset, we have plotted the radial profiles for the whole tetra-(oxyethylene) part (purple), dodecane chain (magenta), the water, and decane.

chains in contact with decane. For the hydrophilic headgroup, only the two outermost EO groups (EO_1 and EO_2) share significant contacts (∼5.0−7.0%) with the oil. For the water, the surface contacts with decane are ∼4.7% and ∼1.3% for RM94t and RM94g respectively, indicating that the micellar water is better confined in RM94g than in RM94t. As expected, the computed density of oil reaches its bulk density value (∼0.72 g/cm^3) at a distance from the micelle, near the edge of the simulation box.

In conclusion, the two computed density profiles obtained for RM94t and RM94g clearly show that the two conformations of the hydrophilic groups yield two different micelles, which differ primarily in their water core structure and localization.

Surfactant Conformation. To gain insights into the surfactant conformation and the water core differences between the two micelles, we study the surfactant chain conformation and its hydration. For this purpose, we have first computed the averaged end-to-end distance probability distribution,[27] i.e. $P(r)$ of the $C_{12}E_4$ total chain, the hydrophobic tail, and the headgroup, labeled in the figure d_{C12E4}, d_{C12}, and d_{EO4}, respectively. These profiles are shown in Figures 6 and 7, and the values obtained for the

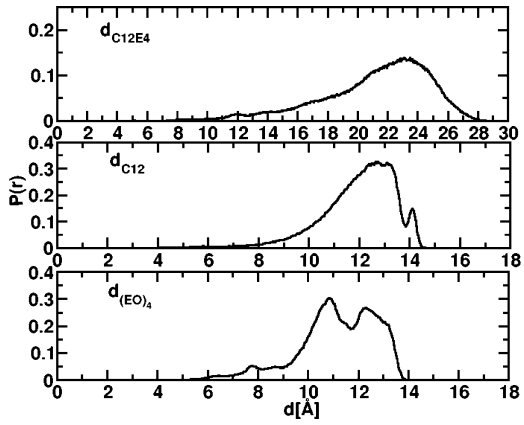

Figure 7. End-to-end distance probability distribution for the RM94t micelle. $P(r)$ are the probability distributions of the following distances: d_{C12E4} between the C_1 and the hydroxyl-oxygen atoms (OH), d_{C12} between C_1 and C_{12} atoms, and d_{EO} between the O_1 and the terminal OH; see Figure 1 localization of these atoms. $P(r)$ is normalized to 1, and a 0.1 Å bin width was used.

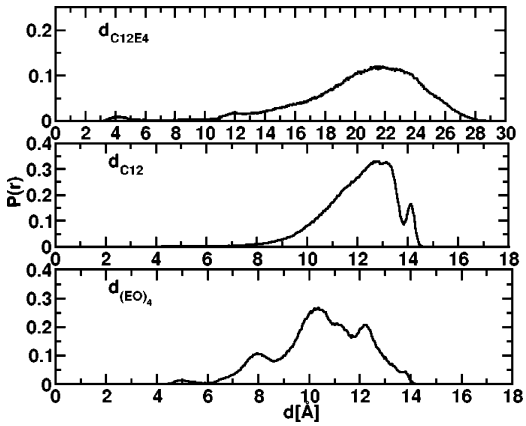

Figure 8. End-to-end distance probability distribution for the RM94g micelle. See legend of the Figure 7 for explanations.

maximum of the d_{C12E4} distribution are reported in Table 4. As we see in Figures 6 and 7, the $P(r)$ for all $C_{12}E_4$ molecules is very broad, indicating a large distribution of the d_{C12E4} lengths for the surfactant in the two micelles. The corresponding $P(r)$ for the d_{C12} functions computed from the distance between the first (C_1) and last carbon (C_{12}) of the dodecyl chain, shows a well-defined peak at ∼12.8 Å for the two RMs. This value is ∼7.2% smaller than that computed for an all trans conformation chain (∼ 13.8 Å) with the DS ViewerPro (Accelrys) modeling program.

For the hydrophilic headgroup length (d_{EO}), the $P(r)$ functions are presented in the lower panels of Figures 7 and 8. They show two broader functions with two intensities at ∼10.5 and ∼12.0 Å (RM94t) and three intensities at ∼8.0, ∼10.3, and ∼12.0 Å (RM94g), indicating a coexistence of two and three populations with different lengths for the surfactant headgroup in our RMs. The first peak in this function shows that d_{EO} is slightly smaller for RM94g (10.3 Å) than for RM94t (10.5 Å). Theses values are significantly smaller than the calculated length for the same headgroup in the "all trans" configuration (∼14.2 Å).[49]

As shown in Table 4 and in Figures 6 and 7, the d_{C12E4} is 6.4% shorter for RM94g (∼21.8 Å) than for RM94t (∼23.3 Å). These distances are found to be, on average, ∼20% smaller than that

(49) Fragneto, G.; Lu, J. R.; McDermott, D. C.; Thomas, R. K.; Rennie, A. R.; Gallagher, P. D.; Satija, S. K. Structure of monolayers of tetraethylene glycol monododecyl ether adsorbed on self-assembled monolayers on silicon: A neutron reflectivity study. *Langmuir* **1996**, *12*(2), 477−486.

Table 5. Average Relative Trans and Gauche Populations (in %) for the CCCC, OCCO, and OCCO Dihedrals in Surfactant[a]

	RM94t			RM94g		
system	p_{g+}	p_t	p_{g-}	p_{g+}	p_t	p_{g-}
CCCC	13.1	74.8	12.1	12.1	74.2	13.7
COCC	16.6	70.0	13.4	23.4	60.4	16.2
$(O_1CCO_2)_1$	20.3	58.0	21.7	0.0	8.5	91.5
$(O_2CCO_3)_2$	28.7	55.3	16.0	4.2	16.0	79.8
$(O_3CCO_4)_3$	26.3	46.3	27.4	5.3	17.0	77.7
$(O_4CCO_h)_4$	47.3	15.0	37.7	52.0	3.0	45.0
OCCO[b]	25.1	53.2	21.7	3.2	13.8	83.0

[a] Here, torsions angles between −120° and 0° were defined to be gauche$^-$ (p_{g-}); those between 0° and +120° as gauche$^+$ (p_{g+}). See Figure 1 for positions of the $(OCCO)_n$ along the surfactant chain. [a] Values obtained by averaging the data for the three first OCCO dihedrals (i.e. $(OCCO)_{1-3}$).

of the same chain in the extended conformation (∼28.0 Å). Since the $P(r)$ functions are strongly related to the surfactant chain conformation, we study in the next paragraph the surfactant chain conformation for the two micelles through their torsion angles.

For the C_mE_n surfactant family, three representative dihedral angle populations have been examined:[18−21,23] the CCCC dihedral angles of the tail backbone and the OCCO and CCOC dihedral angles in the EO part. The CCCC dihedral populations (p) of the C_{12} is mostly in the trans state (p_t) with a relative population p_t ≈75.0%, in agreement with other simulations[18−21,23] and consistent with the small values of d_{C12} (compared to the "all trans" conformation) calculated previously.

In Table 5, we have reported the relative average populations of the OCCO and CCOC dihedral angles for the headgroup. As reported,[18,21] only dihedrals in the three first EO units (i.e. EO_{1-3}) have been considered here, i.e., four COCC and three OCCO dihedrals per chain. The CCOC average distribution shows that these angles are mainly in the trans conformation with a relative population RM94t ($p_{g+} = 16.6\%$, $p_t = 70.0\%$, and $p_{g-} = 13.4\%$) and RM94g ($p_{g+} = 23.4\%$, $p_t = 60.4\%$, and $p_{g-} = 16.2\%$) as reported in previous simulations of C_mE_n in different surfactant phases.[33,23,50]

For the OCCO torsion angles, in the case of the RM94t initially modeled with a headgroup part in an extended configuration, we observe a small preference of OCCO dihedrals to stay in the trans state conformation with relative populations: $p_{g+} = 25.1\%$, $p_t = 53.2\%$, and $p_{g-} = 21.7\%$. This contrasts with the RM94g angle conformations, which are not significantly modified, compared to their initial ones. These results suggest that the poor hydration of the surfactant headgroup in our RM stabilizes the OCCO torsion angle conformation. Indeed, for ionic surfactants with a headgroup fully accessible to water, other simulations[16,18−23] have shown that these angles are mostly in gauche^{+-} state.

In Table 5, we have listed the relative population of the gauche/trans states of the three OCCO angles of the head units. As shown in this Table, the relative gauche^{+-} population of the OCCO dihedrals increases slightly with the proximity of these angles to the water pool: The first OCCO torsion is found to be mostly in the trans state, whereas the third and the fourth OCCO are mainly gauche^{+-}.

For the RM94g micelle, the average population for the $(OCCO)_{1-3}$ angles is found to be mostly in gauche^{+-} states with a preference for the gauche$^-$ conformation ($p_{g+} = 3.2\%$, $p_t = 13.8\%$, and $p_{g-} = 83.0\%$). The relative populations of these dihedrals are close to the initial configuration given to the headgroup.

In contrast to other simulations in the literature,[16,18−23] we found that the outermost dihedrals near the water pool (see second last row in Table 5) (i.e. the $(OCCO)_4$) have a strong preference for the gauche^{+-} state with close relative populations for the two micelles studied.

Table 6. Average Number of Nearest Neighbors for Ether-Oxygen (O_n) and Hydroxyl-Oxygen Atoms (O_h) with Water (O_w)[a]

$n_w^{EO\,b}$	RM94t	RM94g
O_1-O_w	0.3	0.1
O_2-O_w	0.5	0.2
O_3-O_w	0.8	0.5
O_4-O_w	0.9	0.6
O_h-O_w	1.7	1.4

[a] See Figure 1 for localization of these atoms in the surfactant chain. [b] The values have been obtained by integrating the pair correlation functions $g(r)$ up to the minimum located at a distance d, after the first peak. $d \sim 3.5$ Å for the O_n-O_w and O_h-O_w.

Further investigations confirm that all OCCO (including the terminal O−C−C−OH) dihedral angles are rigid during the 3 ns simulation time. Indeed, computation of the number of trans → gauche^{+-} transitions per nanoseconds and per dihedral (N_{tr}) shows that the N_{tr} for the three first OCCO torsion angles of the two micelles are close to 0, whereas for O−C−C−OH $N_{tr} \sim 1.0$ ns^{-1}. These findings are in agreement with the observations of Tasaki[16] where the OCCO dihedrals in PEO chain fully hydrated (in particular for the internal C−C bonds) were found very stable at room temperature with a long relaxation time. In our micelles because of the confinement effects of the water pool, we do not expect to observe large changes in OCCO dihedrals and in particular for those far away from the water pool even for longer accessible simulation times.

Hydration of the Surfactant Headgroup. To gain insights on the differences in the headgroup hydration of the two RMs, we have computed the radial pair density functions $g(r)$ of the water oxygen with the ether-oxygen atoms and the hydroxyl-oxygen atoms of the EO_4 group. These functions (not shown) present two strong peaks at ∼ 2.8 Å and at ∼4.7 Å. For the two micelles studied, the intensity of these peaks is increased by the proximity of the ether-oxygen atoms to the water pool.

The average number of water molecules bound to the first shell of each ether-oxygen (n_w^{EO}) was computed by integrating the $g(r)$ until ∼3.5 Å, which, on average, corresponds to the function minimum, following the first peak. The hydration number values are presented in Table 6. To gather a "global" picture of the ether-oxygen hydration, we have first estimated the average number of water per EO unit, $\langle n_w^{EO} \rangle$ and found that $\langle n_w^{EO} \rangle = 0.6$ and $\langle n_w^{EO} \rangle = 0.3$ for RM94t and RM94g, respectively. These results indicate that the gauche conformation of the headgroup lowers the hydration of the headgroup, on average, by a factor of 2. These values are, as expected, lower than the $\langle n_w^{EO} \rangle$ found for a long PEO chain in water[16] ($\langle n_w^{EO} \rangle \sim 2.9$) or for a $C_{12}E_3$ direct micelle [21] ($\langle n_w^{EO} \rangle = 2.8$) fully solvated in water. For a $C_{12}E_4$−water−decane system with a water−surfactant ratio close to ∼11 (near a lamellar phase[5]), Ravey et al.[45] estimated the number of water per EO unit close to 2.5, much larger than our values.

Since in our RM headgroup ether-oxygens have a different accessibility to water, we have also examined the "local" hydration of each EO unit (n_w^{EO}) as a function of its distance to the water pool. These values are reported in the first four rows of Table 6. The values obtained confirm, as previously noticed with the radial mass profiles, that water penetrates more deeply in the

(50) Chanda, J. S. B. Molecular Dynamics Study of a Surfactant Monolayer Adsorbed at the Air/Water Interface. *J. Chem. Theory Comput.* **2005**, *1* (5), 963−971.

headgroup in RM94t than in RM94g. Indeed, the n_w^{EO} increases gradually with the proximity of the group to the water pool. We found that the number of water molecules in the first shell of the first EO group (EO_1, the outermost oxyethylene group of the headgroup, near the dodecyl chain) is small, close to ~0.3 (RM94t) and ~0.1 (RM94g). It increases to ~0.9 for the last EO (EO_4) group (0.6 for RM94g). Nonuniform hydration along the EO chain has been also demonstrated experimentally by Caldararu et al.[12] or Caragheorgheopol et al.[51] for $C_{12}E_4$-RMs in cyclohexane and decane with fluorescence spectroscopy with different probes.

For hydration of the hydroxyl group (O_h), there are on average ~1.7 and ~1.4 water molecules near each hydroxyl-oxygen atom (O_h) for RM94t and RM94g, respectively. These values are similar to those reported by Allen et al.[33] for a $C_{12}E_2$ RM (1.7), but they are lower than those obtained for a $C_{12}E_2$ in a lamellar phase[20] near the CMC (2.0) and much smaller than the value for a single PEO chain fully solvated in water[16] (~3.5). Similar values for RM94t and the $C_{12}E_2$ RM indicate a similar accessibility of O_h group to the water. The low values of the hydration number for the innermost EO units confirm the absence of a bulklike water pool in the micelles interiors.

We also have also examined the hydrogen bond (HB) network between the ether oxygen atoms and water. For a single PEO chain in water, it has been shown that water can form three different types of HB (i): with only one ether-oxygen, (ii) between two ether-oxygen atoms in an adjacent unit (i.e. EO_n and EO_{n+1}), and (iii) with two ether-oxygen atoms connecting two units apart (EO_n and EO_{n+2}).[52] To examine the HB bridges between water and ether-oxygen in our micelles, we have used an geometrical criterion.[53] In our micelles, in agreement with the low hydration of headgroup, none of the preceding HB types have been detected between the water and the ether-oxygen of the $(EO)_{1-3}$ units, and the only HB is between water and the ether-oxygen $(EO)_4$ and the hydroxyl-oxygen.

The average number of HB between water and the OH terminal group of the surfactant (n^{OH}_{HB}) has been also computed. We found $n^{OH}_{HB} = 1.3 \pm 0.1$ and $n^{OH}_{HB} = 1.0 \pm 0.1$ for RM94t and RM94g, respectively. These values are ~2.6 times smaller than that obtained par Sterpone et al.[21] for the $C_{12}E_3$ micelle in water ($n^{OH}_{HB} = 2.8$) or by Tasaki[16] ($n^{OH}_{HB} = 2.6$) for a PEO chain fully hydrated. As for the other HB types, the low number of HB between water and the OH group is probably due to the small number of water molecules in the first shell.

Dynamics of the Water Core. To examine the micellar water dynamic behavior in the micelles, we have calculated the mean square displacement (MSD), or $\langle |r(t)|^2 \rangle$ vs time and compared with the results obtained for SPC bulk water. These functions are displayed in Figure 9. We can see the water diffusion in both micellar cores is smaller than the bulk and present a subdiffusive regime,[54,55] as previously observed for confined water in AOT reverse micelles[27] or for water near the protein surface.[56] This subdiffusive regime is fitted with the power law:

$$\langle |r(t)|^2 \rangle \propto t^{\alpha} \qquad (4)$$

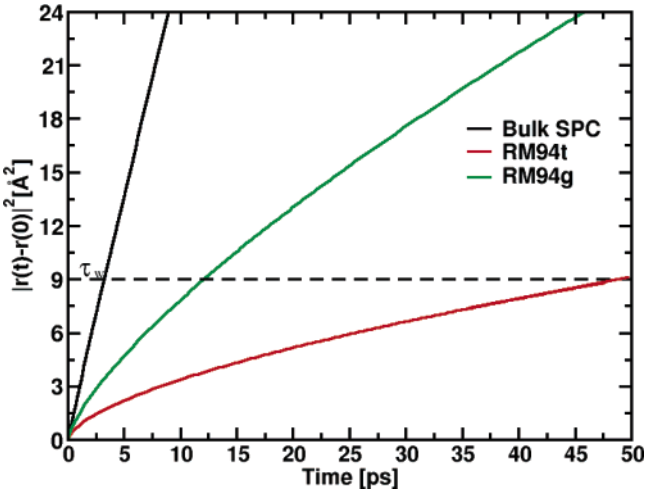

Figure 9. Time evolution of the mean square displacement of the water oxygen versus time for RM94t, RM94g, and bulk water. The dashed line gives the distance for computing the residence time. See the main text.

Table 7. Translational Diffusion of the Micellar Water[a]

system	RM94t	RM94g	bulk
α	0.61	0.73	0.98
τ_w	48.3	12.2	3.3
τ_w/τ_w^b	14.6	3.7	1.0

[a] α is the dispersion regime parameter obtained by fitting the $\langle |r(t)|^2 \rangle$ to t^{α} in Figure 9. τ_w is the water residence time, defined as the time (in ps) for a water to cover its own diameter (i.e. 3 Å). [b] τ_w/τ_w is the ratio between the water residence time in the micelle and bulk water and expresses the retardation compared to bulk water.

For RM94t, α is found smaller ($\alpha = 0.61$) than for RM94 g ($\alpha = 0.73$). For a nonlinear diffusion, it is useful to compute the water residence time, τ_w, and to compare it to the water bulk value, τ_w^b. τ_w is defined as the time required by a molecule to cover is own diameter, which is ~3 Å for water.[56] In Table 7, we present the diffusion parameters in RMs and bulk water. For RM94t where the surfactant headgroup is mainly trans and the water is more trapped in the polyoxyethylene chain, the water residence time is found to be 14.6 times smaller than that of the bulk.

In RM94g, water diffusion is much faster than in RM94t with a water retardation, the ratio τ_w/τ_w^b, only 3.7. As shown previously by experimental techniques such as fluorescence probe spectroscopy,[12,13,57] NMR, ESR, and near-infrared spectroscopic studies,[58] water starts to form bulklike water pool in $C_{12}E_4$ RMs for $W_o \approx 4.5$. Below this value water molecules are thought to be mainly trapped in the polyoxethylene group[13,15] and strongly restricted in their movements. We have computed the average percentage of water molecules inside the first shell (i.e. $r \leq 3.5$ Å) of ether-oxygen and of the termini hydroxyl oxygen atoms. We found that in RM94t about ~80% of the water molecules are trapped in the first shell of the polar group of the surfactant whereas in RM94g this value is close to 29%. Thus, these results

(51) Caragheorgheopol, A.; Pilar, J.; Schlick, S. Hydration and Dynamics in Reverse Micelles of the Triblock Copolymer $EO_{13}PO_{30}EO_{13}$ in Water-Xylene Mixtures: A Spin Probe Study. *Macromolecules* **1997**, *30* (10), 2923−2933.

(52) Wahab, S. A.; Harada, T.; Matsubara, T.; Aida, M. Quantum Chemical Study of the Interaction of the Short-Chain Poly(oxyethylene)s $CH_3(OCH_2CH_2)$-$mOCH_3$(C_1E_mC.; m = 1 and 2) with a Water Molecule in the Gas Phase and in Solutions. *J. Phys. Chem. A* **2006**, *110* (3), 1052−1059.

(53) Luzar, A.; Chandler, D., Structure and hydrogen bond dynamics of water-dimethyl sulfoxide mixtures by computer simulations. *J. Chem. Phys.* **1993**, *98* (10), 8160−8173.

(54) Christensen, M.; Pedersen, J. B. Diffusion in inhomogeneous and anisotropic media. *J. Chem. Phys.* **2003**, *119* (10), 5171−5175.

(55) Bagchi, B. Water dynamics in the hydration layer around proteins and micelles. *Chem. Rev.* **2005**, *105* (9), 3197−3219.

(56) Marchi, M.; Sterpone, F.; Ceccarelli, M. Water Rotational Relaxation and Diffusion in Hydrated Lysozyme. *J. Am. Chem. Soc.* **2002**, *124* (23), 6787−6791.

(57) Correa, N. M.; Biasutti, M. A.; Silber, J. J. Micropolarity or Reversed Micelles: Comparison between Anionic, cationic, and Nonionic Reversed Micelles. *J. Colloid Interface Sci.* **1996**, *184* (2), 570−578.

(58) Kawai, T.; Shindo, N.; Kon No, K. Solubilized states of water and formation of reversed micelles in polyoxyethylated nonylphenyl ethers in cyclohexane media. *Colloid Polym. Sci.* **1995**, *273* (2), 195−199.

(59) DeLano, W. L. *The PyMOL Molecular Graphics System*, ver. 0.99; DeLano Scientific: San Carlos, CA, 2002.

indicate that RM94t is the best realistic model of $C_{12}E_4$ reverse micelle at $W_o = 3$.

IV. Conclusions

This paper reports two molecular dynamic simulations of $C_{12}E_4$ reverse micelles with a water-to-surfactant molar ratio of 3 in decane. We investigated the effect of the two possible conformations (trans vs gauche) for the tetraoxyethylene part of the surfactant on the RM structures and the inner water dynamics.

To study the effect of the surfactant conformation on the micelles, we have extensively examined their structural and dynamical properties and then compared with data from the literature. We find that both simulated micelles have a nonspherical shape with an eccentricity factor close to 0.59, compatible with published experimental observations.[5] The shapes of both micelles are not affected by the surfactant headgroup conformation; in contrast the structural and diffusional properties of the micellar water do depend of the conformation of the $C_{12}E_4$ headgroups.

Comparison of various micellar properties (such as water size, surface area per surfactant headgroup, hydration gradient of the hydrophilic chain, and water dynamics) between the two micelles shows that those micelles with a surfactant chain initially modeled in trans reproduce better the experimental structures. Indeed, when the hydrophilic part of the $C_{12}E_4$ is modeled with the gauche (i.e. helix) structure, we observe that the water-related structural and dynamic properties are far from the experimental data.

Many experimental studies[5,12,13,15,57] suggest that in $C_{12}E_4$ RMs surfactant headgroups adopt an extended conformation which favors the micellar water entrapment. Our MD results demonstrate that the headgroup in trans conformation is the best model of $C_{12}E_4$ reverse micelles.

Our MD studies thus give an interesting picture of the effect of low hydration and the restricted environment on the structure of a molecular system (such as RMs). The results obtained in these simulations have been of course carried out at a low water content. Future investigations will focus on extending our modeling to larger $C_{12}E_4$/decane micelles with increased size of water pool.

Acknowledgment. S.A. thanks Dr. Fabio Sterpone for illuminating discussions and his help during the early stages of this work.

Note Added after ASAP Publication. This article was published ASAP on September 21, 2006. A value in Table 4 has been changed. The correct version was reposted on September 21, 2006.

LA060978V